

This is the accepted manuscript made available via CHORUS. The article has been published as:

Large and homogeneous mass enhancement in the rattling-induced superconductor $\text{KOs}_{2}\text{O}_{6}$

Taichi Terashima, Nobuyuki Kurita, Andhika Kiswandhi, Eun-Sang Choi, James S. Brooks, Kota Sato, Jun-ichi Yamaura, Zenji Hiroi, Hisatomo Harima, and Shinya Uji

Phys. Rev. B **85**, 180503 — Published 17 May 2012

DOI: [10.1103/PhysRevB.85.180503](https://doi.org/10.1103/PhysRevB.85.180503)

Large homogeneous mass enhancement in the rattling-induced superconductor KOs_2O_6

Taichi Terashima,¹ Nobuyuki Kurita,¹ Andhika Kiswandhi,² Eun-Sang Choi,² James S. Brooks,² Kota Sato,³ Jun-ichi Yamaura,³ Zenji Hiroi,³ Hisatomo Harima,⁴ and Shinya Uji¹

¹*National Institute for Materials Science, Tsukuba, Ibaraki 305-0003, Japan*

²*National High Magnetic Field Laboratory, Florida State University, Tallahassee, FL 32310, USA*

³*Institute for Solid State Physics, University of Tokyo, Kashiwa, Chiba 277-8581, Japan*

⁴*Department of Physics, Graduate School of Science, Kobe University, Kobe, Hyogo 657-8501, Japan*

(Dated: May 9, 2012)

We have determined the Fermi surface in KOs_2O_6 ($T_c = 9.6$ K and $B_{c2} \sim 32$ T) via de Haas-van Alphen (dHvA) oscillation measurements and a band structure calculation. We find effective masses up to $26(1) m_e$ (m_e is the free electron mass), which are unusually heavy for compounds where the mass enhancement is mostly due to electron-phonon interactions. Orbit-resolved mass enhancement parameters λ_{dHvA} are large but fairly homogeneous, concentrated in the range 5 – 8. We discuss origins of the large homogeneous mass enhancement in terms of rattling motion of the K ions.

PACS numbers: 71.18.+y, 74.70.Dd, 74.25.Kc, 63.20.kd

The alkali-metal osmium oxides AOs_2O_6 ($A = \text{K, Rb, and Cs}$)^{1–3} crystallize in the cubic β -pyrochlore structure with space group $Fd\bar{3}m$ (No. 227).^{4–6} The A ion is enclosed in an oversized cage formed by OsO_6 octahedra and vibrates in an anharmonic potential with a flat bottom, giving rise to nearly-localized low-energy anharmonic phonon modes,⁷ i.e., rattling modes.⁸ The anharmonicity grows with reducing the ionic size from Cs to K, and an unusually large atomic displacement parameter $U_{iso} = 0.074 \text{ \AA}$ has been found for the K atom by an x-ray structural analysis of KOs_2O_6 .⁴ Existence of low-energy rattling modes in AOs_2O_6 is further evidenced by various measurements. Analyses of specific heat data indicate inclusion of Einstein modes representing rattling modes in addition to usual Debye and electronic terms is necessary to model the specific heat in AOs_2O_6 .^{9–11} The estimated Einstein temperatures are $\theta_E = 22$ and 61 K for $A = \text{K}$, 66.4 K for Rb, and 75.1 K for Cs.^{10,11} The convex upward temperature dependence of resistivity^{10,11} and phonon-dominated NMR relaxation rates at the K site in KOs_2O_6 ¹² have been accounted for by considering the rattling.¹³ Moreover, the rattling modes have directly been observed in laser photoemission spectroscopy (PES),¹⁴ Raman scattering,^{15–17} and inelastic neutron scattering.¹⁸ Finally, a mysterious first-order isomorphous phase transition observed only in KOs_2O_6 at $T_p = 7.6 \text{ K}$ has been considered to be related to the rattling.^{19–21}

The Sommerfeld coefficients γ of the specific heat are estimated to be $70, 44.7$, and $41.4 \text{ mJK}^{-2}\text{mol}^{-1}$ for $A = \text{K, Rb, and Cs}$, respectively, yielding large mass enhancement parameters $\langle\lambda\rangle$ ($= \gamma/\gamma_{band} - 1$) of $6.3, 3.38$, and 2.76 .^{10,11} It is generally assumed that $\langle\lambda\rangle$ due to electron-phonon interactions can not be very large. However, since enhancement of the magnetic susceptibility in AOs_2O_6 is nearly absent,^{10,11,22} the observed mass enhancement is mostly due to the electron-phonon interactions, including electron-rattling ones. As one goes from Cs to K, $\langle\lambda\rangle$ approximately doubles. The lattice as well as electronic structure of the two compounds ($A = \text{K and Cs}$) is basically the same. The only significant difference is enhanced rattling motion of K in KOs_2O_6 . It can therefore be inferred that at least about half of $\langle\lambda\rangle$ in KOs_2O_6 is ascribed to the electron-rattling interactions.

AOs_2O_6 exhibits superconductivity below the transition temperatures of $T_c = 9.6, 6.3$, and 3.3 K for $A = \text{K, Rb, and Cs}$, respectively.^{1–3} Results of specific heat,^{9–11} penetration depth,^{23–25} thermal conductivity,²⁶ NMR,^{12,27} PES,¹⁴ and scanning tunneling spectroscopy²⁸ measurements indicate fully-gapped s -wave superconductivity, compatible with a phonon origin of the superconductivity, possibly with moderate gap anisotropy (at most $\sim 50\%$). The specific heat jump ΔC at T_c grows from $A = \text{Cs}$ to K, where $\Delta C/\gamma T_c$ of 2.87 indicates very strong coupling.^{10,11} The characteristic phonon energies ω_{in} contributing to the superconductivity have been estimated from the thermodynamic critical fields using a strong-coupling formula and are in good agreement with the energies of the rattling mode θ_E (for $A = \text{K}$, the higher energy of $\theta_E = 61 \text{ K}$ is used).^{10,11} This provides strong evidence that the rattling mode dominates the superconducting Cooper pairing. The electron-phonon coupling constant relevant to the superconductivity λ_{SC} has been estimated from a linear relation of λ_{SC} and T_c/ω_{in} : $\lambda_{SC} = 1.8, 1.33$, and 0.78 for $A = \text{K, Rb, and Cs}$, respectively.^{10,11} The large differences between $\langle\lambda\rangle$ and λ_{SC} are intriguing.

In this Rapid Communication, we determine the Fermi surface in KOs_2O_6 via de Haas-van Alphen (dHvA) measurements and an electronic band structure calculation. We find large effective masses up to $26(1) m_e$ (Table I, m_e is the free electron mass). Such heavy masses are rare except for lanthanide or actinide-based heavy-fermion compounds. Orbit-resolved mass enhancement parameters λ_{dHvA} ($= m^*/m_{band} - 1$) are in the range $5\text{--}8$, consistent with the specific-heat $\langle\lambda\rangle$. It is often argued that phonon-mediated superconductors with relatively high T_c owe their high T_c to strong coupling between particular phonons and particular electronic states, which will generally leads to large variation in the mass enhancement over the Fermi surface.^{29–32} However, by comparison with $\text{LuNi}_2\text{B}_2\text{C}$ and MgB_2 , we show that the mass enhancement in KOs_2O_6 can be described as fairly homogeneous over the Fermi surface.

The KOs_2O_6 single crystal, roughly $(0.2 \text{ mm})^3$, used in this study was synthesized from mixture of KOsO_4 and Os as described in Ref. 10, where a residual resistivity ratio of about 300 was found for a similarly synthesized single crystal. dHvA oscillations in magnetic torque were detected using a piezoresistive microcantilever. A dilution refrigerator installed in a resistive magnet was used to produce temperatures T down to 0.03 K in magnetic fields B up to 35.1 T . The field was rotated in the $(1\bar{1}0)$ plane, and the field direction θ is measured from the $[001]$ axis [inset of Fig. 1(a)]. The band structure of KOs_2O_6 was calculated within the local-density approximation using a full-potential linearized augmented plane wave (FLAPW) method (TSPACE and KANSAL-06). The obtained band structure is consistent with previous calculations^{7,33–35} and is very similar to that of CsOs_2O_6 .³⁶ Two bands cross the Fermi level, giving rise to the hole and electron sheets of the Fermi surface [Fig. 2(b)].

Figure 1(a) shows magnetic torque in KOs_2O_6 for $\theta = 79^\circ$. The field-up and field-down curves separate at a field between 31 and 32 T . Although the field thus defined is the irreversibility field, it is comparable to $B_{c2} = 30.6 \text{ T}$ ³⁷ or 33 T ³⁸ determined from penetration depth and resistivity measurements and hence we identify it with B_{c2} . dHvA oscillations are clearly visible and continue below B_{c2} similarly to many other type-II superconductors.^{39–41} Slight difference in the oscillation phase between the up and down sweeps, which becomes apparent for $B \lesssim B_{c2}$, is not *intrinsic*. It is not reproducible and is due to some experimental problem.⁴² The Fourier transforms [Fig. 1(b)] show several fundamental frequencies, labeled with Greek letters, and their harmonics and combinations. The temperature dependence of the amplitude of the frequency ρ is shown in the inset. A fit to the standard Lifshitz-Kosevich formula⁴³ (solid curve) indicates the associated effective mass of $26(1) m_e$.

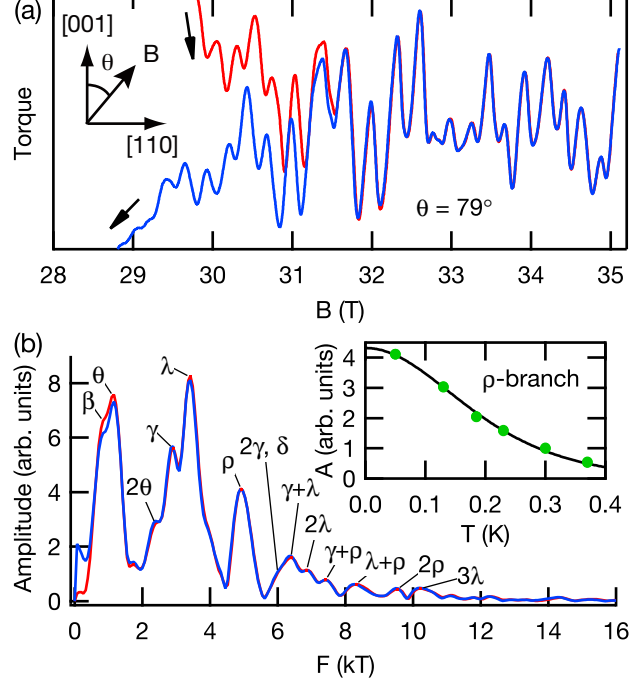


FIG. 1. (color online). (a) Magnetic torque in KOs_2O_6 at $T = 0.05$ K for the field direction $\theta = 79^\circ$. Both field-up and field-down sweeps are shown. Slight difference in the oscillation phase between the up and down sweeps for $B \lesssim 32$ T is *not intrinsic* but due to some experimental problem. (b) Corresponding Fourier transforms in $1/B$ for a field range 30.9–35.1 T, which gives a frequency resolution of $\Delta F = 258$ T. Fundamental dHvA frequencies labeled with Greek letters and their harmonics and combinations are resolved. (inset) T -dependence of the amplitude A of the frequency ρ . The associated effective mass m^* is estimated to be $26(1) m_e$ from a fit to the standard Lifshitz-Kosevich formula (solid curve).

TABLE I. Experimental and calculated dHvA frequencies and effective masses.

θ ($^\circ$)	Branch	Experiment		Calculation		λ_{dHvA}
		F (kT)	m^*/m_e	F (kT)	m_{band}/m_e	
7	β	0.6 ^a	4.7(3) ^a	0.6	0.56	7.3(5)
7	γ	3.0	11.5(6)	2.8	1.91	5.0(3)
7	δ	6.5	14.5(9)	5.9	1.89	6.7(5)
7	ϵ	10.7	20(2)	10.4	3.30	5.0(6)
45	β	0.9	9.2(7)	0.9	1.03	7.9(7)
45	θ			1.4	1.40	
45	θ	2.0		1.8	1.67	
45	γ	2.8	14(1)	2.5	1.73	7.0(6)
45	ζ			4.1	3.13	
45	δ	5.9	15(1)	5.2	2.03	6.5(5)
79	β	0.8	8.4(9)	0.9	1.01	7.3(9)
79	θ	1.1	8.8(8)	1.1	0.997	7.8(8)
79	ν			1.8	1.73	
79	γ	2.9	14(2)	2.7	1.97	5.8(6)
79	λ	3.4	20(2)	3.5	3.11	5.3(5)
79	ρ	4.9	26(1)	4.8	3.72	6.0(3)
79	δ			5.4	2.29	

^a Estimated from the second harmonic oscillation.

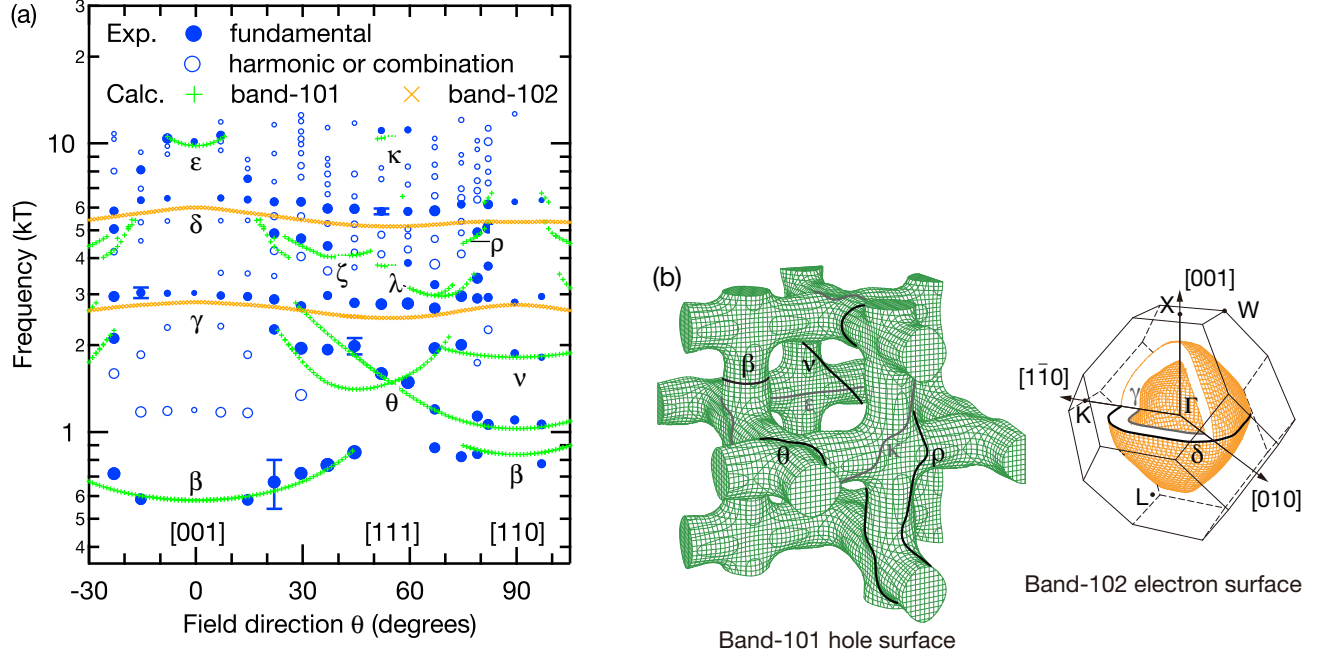


FIG. 2. (color online). (a) Angular dependences of the experimental and calculated dHvA frequencies. For the experimental ones, those assigned to fundamentals are shown by solid circles, while those assigned to harmonics or combinations are shown by open circles. The mark sizes are based on the oscillation amplitudes logarithmically. Error bars attached to some data points are based on half of the frequency resolution, i.e., ± 129 T. (b) Calculated Fermi surface of KOs₂O₆. The hole surface (left) is shown in the repeated zone scheme. Orthogonal pillars constituting the hole surface cross at X points. The observed dHvA orbits are shown in the figures except for the ζ and λ orbits, both of which are orbits on the hole surface. ζ is a V-shaped orbit extending from an X point toward adjacent X points along the k_x and k_y directions. λ is centered approximately at a middle of two vertically adjacent X points and extends between the two X points.

Figure 2(a) compares the angular dependences of the experimental and calculated dHvA frequencies, and Fig. 2(b) explains observed orbits including the heaviest-mass orbit ρ . In our previous work,²² when the lowest temperature was 0.6 K, we could observe only one frequency branch, β , while we have observed nearly the entire Fermi surface in this study owing to much lower measurement temperatures. The agreement between the experimental and calculated frequencies is satisfactory. Both δ and γ frequencies are slightly larger than calculated as in CsOs₂O₆,³⁶ but this can not be resolved by a rigid band shift. If the electron band is shifted up, for example, δ decreases while γ increases. Accordingly, we have tried no adjustment to the calculation.

We note one noticeable difference between the Fermi surfaces of KOs₂O₆ and CsOs₂O₆. In the case of CsOs₂O₆, there are through holes connecting the inner and outer sheets of the electron surface along the $\langle 111 \rangle$ directions,³⁶ while in KOs₂O₆ there are no through holes and hence the inner and outer sheets are disconnected.

Table I lists the fundamental frequencies and effective masses for the three field directions where the temperature dependence was measured. Large effective masses up to 26(1) m_e and the orbit-resolved dHvA mass enhancement parameters λ_{dHvA} of 5–8 are observed. A comparably heavy mass of 22 m_e was previously reported for a filled skutterudite compound LaFe₄P₁₂,⁴⁴ where rattling motion of La is expected.⁴⁵

Near absence of the Stoner enhancement and hence of the electronic mass enhancement in AOs₂O₆ has been evidenced by the following: (1) The magnetic susceptibilities, which are nearly temperature independent, are almost the same for the three compounds ($A = \text{K, Rb, and Cs}$) despite a factor of about two variation in their mass enhancements.^{10,11} (2) The Pauli paramagnetic susceptibilities, which are estimated by correcting the measured susceptibilities for the core and orbital contributions, match the band values within 30%.^{10,11} (3) The large B_{c2} of over 30 T in KOs₂O₆ is incompatible with a significant Stoner enhancement, which would reduce B_{c2} .²² The large mass enhancements are therefore for the most part due to the electron-phonon and electron-rattling interactions.

The heaviest mass found in CsOs₂O₆ is only 12 m_e and λ_{dHvA} is in the range 2.0–3.8.³⁶ The mass enhancements are approximately doubled from Cs to K because of the enhanced rattling in KOs₂O₆, and hence roughly half of the mass enhancements in KOs₂O₆ can be ascribed to the electron-phonon interactions as already mentioned in the introduction. It is interesting to note that electron-phonon coupling λ_{ep} estimated from band structure calculations is

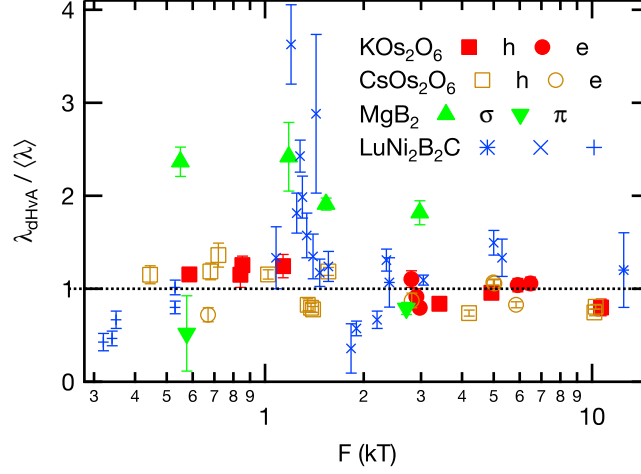


FIG. 3. (color online). Orbit-resolved dHvA mass enhancement parameters λ_{dHvA} in KOs_2O_6 normalized to the Fermi-surface averaged specific-heat mass enhancement parameter $\langle\lambda\rangle$ as a function of the dHvA frequency. Data for CsOs_2O_6 ,^{11,36} $\text{LuNi}_2\text{B}_2\text{C}$,^{46,47} and MgB_2 ^{48,49} are shown for comparison. Different symbols are used for different bands as indicated by the legend in the figure.

about 0.8 for all the three compounds ($A = \text{K, Rb, and Cs}$)³⁴ and hence is strikingly inconsistent with the experimental observations.

The determined dHvA mass enhancement parameters λ_{dHvA} are normalized to the Fermi-surface averaged mass enhancement parameter $\langle\lambda\rangle$ from the specific heat¹⁰ and are plotted as a function of the dHvA frequency in Fig. 3. The figure also shows data for CsOs_2O_6 ,^{11,36} $\text{LuNi}_2\text{B}_2\text{C}$,^{46,47} and MgB_2 .^{48,49} Data points for different bands (Fermi surface sheets) are shown by different symbols. In the case of MgB_2 , the disparity between the σ and π bands is evident: $\lambda_{dHvA}/\langle\lambda\rangle \approx 2$ for the σ bands (upward triangles), while $\lambda_{dHvA}/\langle\lambda\rangle < 1$ for the π bands (downward triangles). This is of course intimately related to the two-gap structure of the superconductivity in MgB_2 : the superconducting energy gap Δ for the σ bands is about three to four times larger than that for the π bands.⁴⁹ In the case of $\text{LuNi}_2\text{B}_2\text{C}$, where three bands cross the Fermi level, variation in the mass enhancements is still larger. The mass enhancement parameters not only differ from band to band but also depend on orbit orientation in one band (see crosses near $F = 1.1\text{--}1.4$ kT distributed in the range $\lambda_{dHvA}/\langle\lambda\rangle = 1.3\text{--}3.6$; these are data points for the same band⁴⁶). The large variation is again related to a highly anisotropic multigap structure with deep minima or possibly nodes.^{39,50,51} In sharp contrast, data points of KOs_2O_6 (and also of CsOs_2O_6) are concentrated in the vicinity of $\lambda_{dHvA}/\langle\lambda\rangle = 1$, and there is no clear distinction between the mass enhancements for the hole (squares) and electron (circles) bands. This homogeneity is compatible with the limited anisotropy of the superconducting gap in AOs_2O_6 .

It is instructive to recall here how the strongly band-dependent λ in MgB_2 arises.³¹ The σ and π bands in MgB_2 have distinct characters: the former are two-dimensional bands derived from B p_{xy} orbitals, while the latter are three-dimensional bands derived from B p_z orbitals. The former strongly couple with the E_{2g} phonon, which is a B-B bond stretching mode, resulting in the large λ only for the σ bands. In contrast, there is no clear difference in character between the hole and electron bands in KOs_2O_6 : both are three dimensional, arising from Os $5d$ and O $2p$ orbitals. Oxygen vibration modes will therefore couple to both bands. Raman scattering measurements have found that those modes in AOs_2O_6 are more or less anharmonic and exhibit strong electron-phonon coupling.^{15,17} They are thus important in explaining large λ in AOs_2O_6 (λ is already unusually large in the Rb and Cs compounds without the K rattling). For the K rattling, since electronic states of the K ion contribute little to the density of states at the Fermi level, the large electron-rattling interaction is not due to direct coupling as in MgB_2 between the K rattling motion and a particular electronic band, as noted in Ref. 33. It is due to the low frequencies of the rattling modes (λ is inversely proportional to relevant phonon frequencies) and hence is basically band independent. Thus strong band dependence of λ is not expected in KOs_2O_6 . In addition, this indirect nature of the electron-rattling interaction is probably an important factor enabling the large mass enhancement to occur without resulting in lattice instability.

For the angular variation of λ , KOs_2O_6 is cubic and hence the angular variation is basically expected to be weak. For the electron-rattling interaction, a more intuitive argument might be made. The K ions sit at high symmetry points and the rattling motion is largely isotropic as evidenced by the K-ion electron density determined by x-ray diffraction.¹⁹ Thus electron scattering by the rattling is basically isotropic, which, combined with the three-dimensional

Fermi surface, gives nearly isotropic mass enhancement over the Fermi surface.

In summary, we have determined the Fermi surface in KOs_2O_6 . We have found the mass enhancement parameters of 5–8, which are unusually large for electron-phonon mass enhancement. At least approximately half of the enhancement is ascribed to the electron-rattling interaction. By comparison with MgB_2 and $\text{LuNi}_2\text{B}_2\text{C}$, we have illustrated the homogeneity of the mass enhancements in KOs_2O_6 and its relation to the relatively homogeneous superconducting gap structure. We have discussed origins of the homogeneity in terms of the electronic band structure and rattling modes.

ACKNOWLEDGMENTS

We thank T. Hasegawa for helpful discussion. This work was supported by a Grant-in-Aid for Scientific Research on Innovative Areas "Heavy Electrons" (No. 23102725) of The Ministry of Education, Culture, Sports, Science, and Technology, Japan. AK and JSB acknowledge support from NSF-DMR 1005293. A portion of this work was performed at the NHMFL, supported by NSF Cooperative Agreement DMR-0654118, the State of Florida, and the U.S. DoE.

-
- ¹ S. Yonezawa, Y. Muraoka, Y. Matsushita, and Z. Hiroi, J. Phys.: Condens. Matter **16**, L9 (2004).
 - ² S. Yonezawa, Y. Muraoka, Y. Matsushita, and Z. Hiroi, J. Phys. Soc. Jpn. **73**, 819 (2004).
 - ³ S. Yonezawa, Y. Muraoka, and Z. Hiroi, J. Phys. Soc. Jpn. **73**, 1655 (2004).
 - ⁴ J. Yamaura, S. Yonezawa, Y. Muraoka, and Z. Hiroi, J. Solid State Chem. **179**, 336 (2006).
 - ⁵ R. Galati, R. W. Hughes, C. S. Knee, P. F. Henry, and M. T. Weller, J. Mater. Chem. **17**, 160 (2007).
 - ⁶ J. Yamaura, Z. Hiroi, K. Tsuda, K. Izawa, Y. Ohishi, and S. Tsutsui, Solid State Commun. **149**, 31 (2009).
 - ⁷ J. Kuneš, T. Jeong, and W. E. Pickett, Phys. Rev. B **70**, 174510 (2004).
 - ⁸ V. Keppens, D. Mandrus, B. C. Sales, B. C. Chakoumakos, P. Dai, R. Coldea, M. B. Maple, D. A. Gajewski, E. J. Freeman, and S. Bennington, Nature **395**, 876 (1998).
 - ⁹ M. Bruhwyler, S. M. Kazakov, J. Karpinski, and B. Batlogg, Phys. Rev. B **73**, 094518 (2006).
 - ¹⁰ Z. Hiroi, S. Yonezawa, Y. Nagao, and J. Yamaura, Phys. Rev. B **76**, 014523 (2007).
 - ¹¹ Y. Nagao, J. Yamaura, H. Ogusu, Y. Okamoto, and Z. Hiroi, J. Phys. Soc. Jpn. **78**, 064702 (2009).
 - ¹² M. Yoshida, K. Arai, R. Kaido, M. Takigawa, S. Yonezawa, Y. Muraoka, and Z. Hiroi, Phys. Rev. Lett. **98**, 197002 (2007).
 - ¹³ T. Dahm and K. Ueda, Phys. Rev. Lett. **99**, 187003 (2007).
 - ¹⁴ T. Shimojima, Y. Shibata, K. Ishizaka, T. Kiss, A. Chainani, T. Yokoya, T. Togashi, X.-Y. Wang, C. T. Chen, S. Watanabe, J. Yamaura, S. Yonezawa, Y. Muraoka, Z. Hiroi, T. Saitoh, and S. Shin, Phys. Rev. Lett. **99**, 117003 (2007).
 - ¹⁵ T. Hasegawa, Y. Takasu, N. Ogita, M. Udagawa, J. Yamaura, Y. Nagao, and Z. Hiroi, Phys. Rev. B **77**, 064303 (2008).
 - ¹⁶ J. Schoenes, A.-M. Racu, K. Doll, Z. Bukowski, and J. Karpinski, Phys. Rev. B **77**, 134515 (2008).
 - ¹⁷ T. Hasegawa, Y. Takasu, N. Ogita, J. Yamaura, Y. Nagao, Z. Hiroi, and M. Udagawa, J. Phys.: Conf. Ser. **150**, 052067 (2009).
 - ¹⁸ H. Mutka, M. M. Koza, M. R. Johnson, Z. Hiroi, J. Yamaura, and Y. Nagao, Phys. Rev. B **78**, 104307 (2008).
 - ¹⁹ J. Yamaura, M. Takigawa, O. Yamamuro, and Z. Hiroi, J. Phys. Soc. Jpn. **79**, 043601 (2010).
 - ²⁰ K. Sasai, M. Kofu, R. M. Ibberson, K. Hirota, J. Yamaura, Z. Hiroi, and O. Yamamuro, J. Phys.: Condens. Matter **22**, 015403 (2010).
 - ²¹ K. Hattori and H. Tsunetsugu, J. Phys. Soc. Jpn. **80**, 023714 (2011).
 - ²² T. Terashima, N. Kurita, A. Harada, K. Kodama, J. Yamaura, Z. Hiroi, H. Harima, and S. Uji, J. Phys. Soc. Jpn. **79**, 083703 (2010).
 - ²³ R. Khasanov, D. G. Eshchenko, D. Di Castro, A. Shengelaya, F. La Mattina, A. Maisuradze, C. Baines, H. Luetkens, J. Karpinski, S. M. Kazakov, and H. Keller, Phys. Rev. B **72**, 104504 (2005).
 - ²⁴ I. Bonalde, R. Ribeiro, W. Brämer-Escamilla, J. Yamaura, Y. Nagao, and Z. Hiroi, Phys. Rev. Lett. **98**, 227003 (2007).
 - ²⁵ Y. Shimono, T. Shibauchi, Y. Kasahara, T. Kato, K. Hashimoto, Y. Matsuda, J. Yamaura, Y. Nagao, and Z. Hiroi, Phys. Rev. Lett. **98**, 257004 (2007).
 - ²⁶ Y. Kasahara, Y. Shimono, T. Shibauchi, Y. Matsuda, S. Yonezawa, Y. Muraoka, and Z. Hiroi, Phys. Rev. Lett. **96**, 247004 (2006).
 - ²⁷ K. Magishi, J. L. Gavilano, B. Pedrini, J. Hinderer, M. Weller, H. R. Ott, S. M. Kazakov, and J. Karpinski, Phys. Rev. B **71**, 024524 (2005).
 - ²⁸ C. Dubois, G. Santi, I. Cuttat, C. Berthod, N. Jenkins, A. P. Petrović, A. A. Manuel, O. Fischer, S. M. Kazakov, Z. Bukowski, and J. Karpinski, Phys. Rev. Lett. **101**, 057004 (2008).
 - ²⁹ W. Weber and L. F. Mattheiss, Phys. Rev. B **25**, 2270 (1982).
 - ³⁰ B. Sadigh and V. Ozoliņš, Phys. Rev. B **57**, 2793 (1998).
 - ³¹ I. Mazin and V. Antropov, Physica C **385**, 49 (2003).
 - ³² A. Sanna, G. Profeta, A. Floris, A. Marini, E. K. U. Gross, and S. Massidda, Phys. Rev. B **75**, 020511 (2007).
 - ³³ R. Saniz, J. E. Medvedeva, L.-H. Ye, T. Shishidou, and A. J. Freeman, Phys. Rev. B **70**, 100505(R) (2004).
 - ³⁴ R. Saniz and A. J. Freeman, Phys. Rev. B **72**, 024522 (2005).
 - ³⁵ Z. Hiroi, J. Yamaura, S. Yonezawa, and H. Harima, Physica C **460-462**, 20 (2007).
 - ³⁶ T. Terashima, S. Uji, Y. Nagao, J. Yamaura, Z. Hiroi, and H. Harima, Phys. Rev. B **77**, 064509 (2008).
 - ³⁷ E. Ohmichi, T. Osada, S. Yonezawa, Y. Muraoka, and Z. Hiroi, J. Phys. Soc. Jpn. **75**, 045002 (2006).
 - ³⁸ T. Shibauchi, L. Krusin-Elbaum, Y. Kasahara, Y. Shimono, Y. Matsuda, R. D. McDonald, C. H. Mielke, S. Yonezawa, Z. Hiroi, M. Arai, T. Kita, G. Blatter, and M. Sigrist, Phys. Rev. B **74**, 220506 (2006).
 - ³⁹ T. Terashima, C. Haworth, H. Takeya, S. Uji, H. Aoki, and K. Kadowaki, Phys. Rev. B **56**, 5120 (1997).
 - ⁴⁰ T. J. B. M. Janssen, C. Haworth, S. M. Hayden, P. Meeson, M. Springford, and A. Wasserman, Phys. Rev. B **57**, 11698 (1998).
 - ⁴¹ N. Doiron-Leyraud, C. Proust, D. LeBoeuf, J. Levallois, J.-B. Bonnemaïson, R. Liang, D. A. Bonn, W. N. Hardy, and L. Taillefer, Nature **447**, 565 (2007).
 - ⁴² Similar phase difference between up and down sweeps were observed in some other field sweeps. The onset fields of the difference were random and we found no correlation with B_{c2} .
 - ⁴³ D. Shoenberg, *Magnetic oscillations in metals* (Cambridge University Press, Cambridge, 1984).
 - ⁴⁴ H. Sugawara, T. D. Matsuda, K. Abe, Y. Aoki, H. Sato, S. Nojiri, Y. Inada, R. Settai, and Y. Ōnuki, Phys. Rev. B **66**, 134411 (2002).
 - ⁴⁵ A still heavier dHvA mass of $81 m_e$ was reported for $\text{PrFe}_4\text{P}_{12}$.⁴⁴ However, in this case, $4f$ -degrees of freedom are most likely involved in the mass enhancement and hence it can not directly be compared with the present case.

- ⁴⁶ B. Bergk, V. Petzold, H. Rosner, S.-L. Drechsler, M. Bartkowiak, O. Ignatchik, A. D. Bianchi, I. Sheikin, P. C. Canfield, and J. Wosnitza, Phys. Rev. Lett. **100**, 257004 (2008).
- ⁴⁷ H. Michor, T. Holubar, C. Dusek, and G. Hilscher, Phys. Rev. B **52**, 16165 (1995).
- ⁴⁸ A. Carrington, P. J. Meeson, J. R. Cooper, L. Balicas, N. E. Hussey, E. A. Yelland, S. Lee, A. Yamamoto, S. Tajima, S. M. Kazakov, and J. Karpinski, Phys. Rev. Lett. **91**, 037003 (2003).
- ⁴⁹ F. Bouquet, R. A. Fisher, N. E. Phillips, D. G. Hinks, and J. D. Jorgensen, Phys. Rev. Lett. **87**, 047001 (2001).
- ⁵⁰ M. Nohara, M. Isshiki, H. Takagi, and R. J. Cava, J. Phys. Soc. Jpn. **66**, 1888 (1997).
- ⁵¹ E. Boaknin, R. W. Hill, C. Proust, C. Lupien, L. Taillefer, and P. C. Canfield, Phys. Rev. Lett. **87**, 237001 (2001).